



This is a repository copy of *Avalanche noise characteristics of thin GaAs structures with distributed carrier generation* .

White Rose Research Online URL for this paper:
<http://eprints.whiterose.ac.uk/907/>

Article:

Li, K.F., Ong, D.S., David, J.P.R. et al. (5 more authors) (2000) Avalanche noise characteristics of thin GaAs structures with distributed carrier generation. IEEE Transactions on Electron Devices, 47 (5). pp. 910-914. ISSN 0018-9383

<https://doi.org/10.1109/16.841220>

Reuse

Unless indicated otherwise, fulltext items are protected by copyright with all rights reserved. The copyright exception in section 29 of the Copyright, Designs and Patents Act 1988 allows the making of a single copy solely for the purpose of non-commercial research or private study within the limits of fair dealing. The publisher or other rights-holder may allow further reproduction and re-use of this version - refer to the White Rose Research Online record for this item. Where records identify the publisher as the copyright holder, users can verify any specific terms of use on the publisher's website.

Takedown

If you consider content in White Rose Research Online to be in breach of UK law, please notify us by emailing eprints@whiterose.ac.uk including the URL of the record and the reason for the withdrawal request.



eprints@whiterose.ac.uk
<https://eprints.whiterose.ac.uk/>

Avalanche Noise Characteristics of Thin GaAs Structures with Distributed Carrier Generation

Kim F. Li, *Member, IEEE*, Duu S. Ong, John P. R. David, *Senior Member, IEEE*, Richard C. Tozer, *Senior Member, IEEE*, Graham J. Rees, Stephen A. Plimmer, Keng Y. Chang, and John S. Roberts

Abstract—It is known that both pure electron and pure hole injection into thin GaAs multiplication regions gives rise to avalanche multiplication with noise lower than predicted by the local noise model. In this paper, it is shown that the noise from multiplication initiated by carriers generated throughout a $0.1\ \mu\text{m}$ avalanche region is also lower than predicted by the local model but higher than that obtained with pure injection of either carrier type. This behavior is due to the effects of nonlocal ionization brought about by the dead space; the minimum distance a carrier has to travel in the electric field to initiate an ionization event.

Index Terms—APD, avalanche multiplication, avalanche noise, GaAs, impact ionization.

I. INTRODUCTION

IN resonant cavity photodetectors a Fabry–Pérot cavity tuned to the absorption wavelength allows the use of a thin absorption region and thus reduces the primary carrier transit time without sacrificing quantum efficiency (QE). Furthermore if a separate multiplication region is also made sufficiently thin, the excess noise can be reduced significantly by nonlocal ionization effects [1]–[3]. Such resonant cavity enhanced, separate absorption and multiplication avalanche photodetectors (RCE-SAM-APD's) have been reported recently with high quantum efficiency and high gain bandwidth product [4], [5].

In SAM structures, both the layer width and the doping must be controlled to high precision. The absorption layer must be fully depleted to maximize the QE, however if the field is too high then multiplication can also occur in this region and the advantage of a separate thin multiplication region is reduced. The effect of distributed carrier generation, and so of “mixed” injection, on the noise characteristics of thin avalanching regions in which nonlocal ionization behavior reduces noise has not been investigated. If no appreciable degradation in noise characteristics occurs under such conditions, then a thin multiplication region could also be used as the absorption region to produce an RCE-combined-absorption-multiplication-APD (RCE-CAM-APD), with a less demanding layer structure.

In this paper, the effects of mixed injection on the multiplication and noise characteristics of a GaAs avalanche region nom-

inally $0.1\ \mu\text{m}$ in width are investigated and compared with the results for pure electron and hole injection. The experimental results are interpreted using a previously reported [2], [6] non-local recurrence theory for uniform avalanche regions which is extended here to treat devices with an arbitrary carrier injection profile.

II. GROWTH AND DEVICE FABRICATION

The structure shown in Fig. 1 was grown as an RCE-APD by metal organic vapor phase epitaxy using C and Si as the p^+ and n^+ dopants and was designed to have a high QE at an incident wavelength of 850 nm. However in this study it is not used in resonance and can be regarded as a $p^+(\text{Al}_{0.5}\text{Ga}_{0.5}\text{As})-i(\text{GaAs})-n^+(\text{Al}_{0.5}\text{Ga}_{0.5}\text{As})$ diode with a thin $\text{Al}_{0.2}\text{Ga}_{0.8}\text{As}$ capping layer. Two GaAs homojunction structures, one p^+-i-n^+ and the other a n^+-i-p^+ were also grown by molecular beam epitaxy on $n^+(p^+)$ (001) GaAs substrates and comprised an $n^+(p^+)$ GaAs buffer, an $n^+(p^+)$ AlAs $0.1\ \mu\text{m}$ etch stop layer, $1\ \mu\text{m}$ of $n^+(p^+)$ GaAs, an undoped GaAs avalanche region of width, $w = 0.1\ \mu\text{m}$ and finally a $1\ \mu\text{m}$ GaAs $p^+(n^+)$ layer. Circular mesa diodes of radius 50–200 μm and with annular top contacts for optical access were fabricated from these layers. Dark current measurements on the RCE-APD devices showed low leakage currents of $\sim 200\ \text{nA}$ at 90% of the breakdown voltage on the 100 μm radius devices.

III. MEASUREMENTS

Avalanche multiplication measurements were performed using a noise measurement system with a center frequency of 10 MHz and a noise effective bandwidth of 4.2 MHz [2]. Carrier injection was provided by 442 nm, 542 nm, or 633 nm lasers focused to a spot onto the top $p^+(n^+)$ capping layer. The excess noise factor, F , was determined from the noise power measurements using the method described previously [2] and was calculated from $F = i_{\text{eq}}/M^2i_p$, where M is the mean multiplication, i_p is the unmultiplied primary photocurrent and i_{eq} is the equivalent photocurrent of the silicon p-i-n diode that produces the same noise power as the device under test.

Light of wavelength 633 nm, to which the $\text{Al}_{0.5}\text{Ga}_{0.5}\text{As}$ p^+ and n^+ layers are almost transparent, was used to produce mixed injection in the RCE-APD. Most carriers generated in the thin $\text{Al}_{0.2}\text{Ga}_{0.8}\text{As}$ p^+ layer, the Bragg mirrors and the substrate recombine before diffusing to the high field region. The 633 nm light is absorbed in the GaAs i -region and generates carriers in a distributed manner throughout this region; only these carriers contribute to multiplication. Illuminating with a He-Cd laser at

Manuscript received January 29, 1999; revised July 19, 1999. This work was supported by EPSRC (U.K.) under Grant GR/L71674. The review of this manuscript was arranged by Editor M. F. Chang.

K. F. Li is with Silicon Systems Ltd (SSL), Dublin 2, Ireland.

D. S. Ong is with the Faculty of Engineering, Telekom University (Multimedia University), 75450 Melaka, Malaysia.

J. P. R. David, R. C. Tozer, G. J. Rees, S. A. Plimmer, K. Y. Chang, and J. S. Roberts are with the Department of Electrical and Electronic Engineering, University of Sheffield, Sheffield S1 3JD, U.K.

Publisher Item Identifier S 0018-9383(00)03397-9.

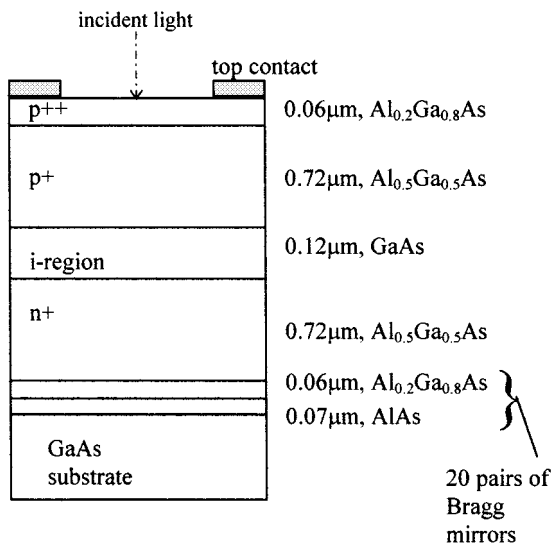


Fig. 1. RCE-APD structure used for mixed carrier initiated multiplication.

442 nm produces nearly pure electron injection since the light is highly absorbed in the $\text{Al}_{0.5}\text{Ga}_{0.5}\text{As}$ p^+ layer and photogenerated minority electrons diffuse to the high field region. For the intermediate incident wavelength of 542 nm some light is absorbed in the p^+ region and some in the i -region resulting in distributed mixed injection with a significant contribution of electrons injected from the p^+ $\text{Al}_{0.5}\text{Ga}_{0.5}\text{As}$ layer. In contrast, in the homojunction GaAs p^+i-n^+ (n^+i-p^+) diodes, light incident at wavelengths of 633 nm, 542 nm, and 442 nm is almost completely absorbed in the $1\ \mu\text{m}$ capping layer producing electrons (holes) that diffuse to the high field region, resulting in pure electron (hole) initiated multiplication.

Fig. 2 shows the multiplication characteristics for the RCE-APD at incident wavelengths of 442 nm, 542 nm, and 633 nm. It can be seen that, for the same reverse bias voltage, the multiplication in the RCE-APD with 442 nm incident light is higher than that at 542 nm which is, in turn, higher than at 633 nm. The GaAs p^+i-n^+ and n^+i-p^+ diodes each produced identical multiplication characteristics with 633 nm, 542 nm and 442 nm incident light and so, for clarity, only the 633 nm multiplication characteristics are shown.

The multiplication characteristics of the RCE-APD at 442 nm are very similar to those of the GaAs p^+i-n^+ diode at 633 nm, suggesting that pure electron initiated multiplication has been achieved. The RCE-APD breakdown voltage is 7 V, identical to that of the $w = 0.1\ \mu\text{m}$ p^+i-n^+ diode, suggesting that although the RCE-APD was grown to a width of nominally $w = 0.12\ \mu\text{m}$ it is closer to $w = 0.1\ \mu\text{m}$. The breakdown voltage of the n^+i-p^+ diode was ~ 6.5 V suggesting that the device is slightly thinner than $0.1\ \mu\text{m}$, as confirmed by analysis of the capacitance voltage measurements and secondary ion beam mass spectroscopy profiles.

Fig. 3 shows plots of excess noise versus multiplication for the RCE-APD and the GaAs p^+i-n^+ (n^+i-p^+) diode together with McIntyre's [8] curves for various values of $k = \beta/\alpha$, where α and β are the electron and hole ionization coefficients, respectively. However, since McIntyre's continuum theory does not

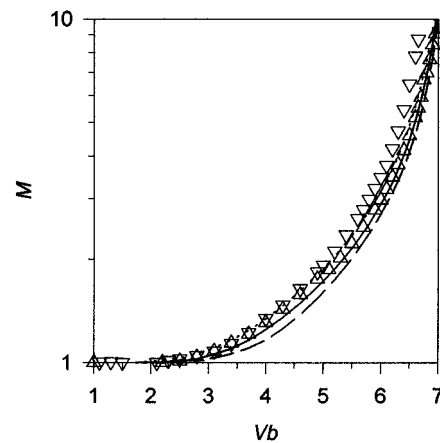


Fig. 2. Multiplication versus reverse bias for the RCE-APD at incident wavelengths of 442 nm (-----), 542 nm (—) and 633 nm (—). Also shown is photomultiplication for pure electron (Δ) and hole (∇) injection in the $0.1\ \mu\text{m}$ GaAs p^+i-n^+ and n^+i-p^+ diodes respectively.

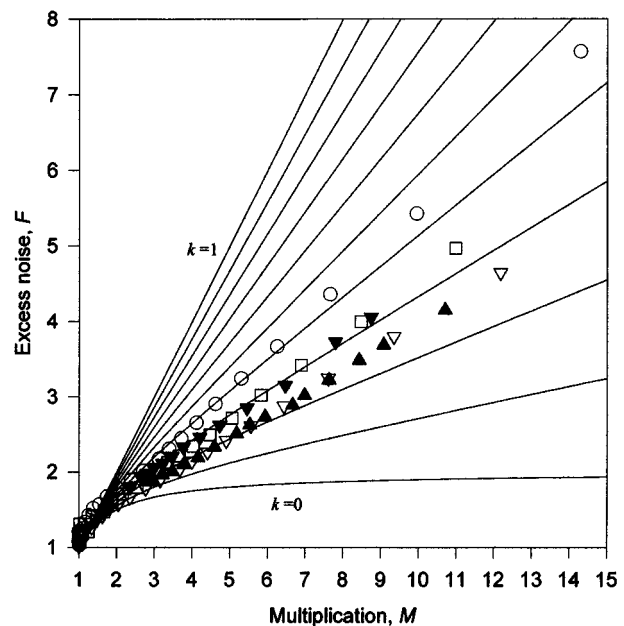


Fig. 3. Excess noise factor versus multiplication for the RCE-APD at incident wavelengths of 442 nm (∇), 542 nm (\square) and 633 nm (\circ), and for the $w = 0.1\ \mu\text{m}$ GaAs p^+i-n^+ (\blacktriangledown) and n^+i-p^+ (\blacktriangle) diodes using 633 nm wavelength light. Solid lines are McIntyre's curves with $k = \beta/\alpha$ increasing from 0 to 1 in steps of 0.1.

apply in the limit of very thin avalanche regions, these curves are included solely for the purposes of comparison.

With 633 nm light incident on the RCE-APD, primary carriers are generated in the high field region and the resulting noise characteristics shown in Fig. 3 correspond approximately to $k \sim 0.4$ in McIntyre's model [8]. For the more energetic incident light of 542 nm and 442 nm the noise characteristics decrease to levels corresponding to $k \sim 0.3$ and $k \sim 0.25$, respectively. Also plotted in Fig. 3 are the pure electron and hole initiated multiplication noise characteristics of the GaAs p^+i-n^+ and n^+i-p^+ diodes using 633 nm light. Unlike in the RCE-APD, illuminating the GaAs p^+i-n^+ (n^+i-p^+) diodes

with 542 nm and 442 nm light produced identical noise characteristics to those obtained with 633 nm excitation. The pure electron injection noise results for the $p^+ - i - n^+$ diode are almost identical to those of the RCE-APD obtained using 442 nm light, further confirming that, as expected, pure electron injection has been achieved in the RCE-APD. However, with 633 nm light and mixed carrier injection, the RCE-APD exhibits noisier characteristics than either the pure electron or pure hole initiated multiplication results.

IV. MODELING

It is worth considering how the gain and excess noise characteristics would behave in thick ($\sim 1 \mu\text{m}$) GaAs structures, where the local model of McIntyre [8] is applicable. At the operating field of such structures $\alpha \approx 2\beta$, and pure electron initiated multiplication, M_e , is greater than pure hole initiated multiplication, M_h . The excess noise results would follow the $k = 0.5$ line in Fig. 3 with electron initiated multiplication (F_e) and the $k = 2$ line with hole initiated multiplication (F_h). For carrier generation within the high field region the gain and excess noise curves would lie between those of M_e and M_h , and between those of F_e and F_h , respectively. In thin GaAs structures, $M_e \sim M_h$ [9] and the slight discrepancies in the $p^+ - i - n^+$ and $n^+ - i - p^+$ multiplication characteristics in Fig. 2 are the result of the slight difference between the avalanche widths. According to the local model when $\alpha \approx \beta$ then $F_e \sim F_h$, corresponding to $k = 1$ in Fig. 3. In this case, distributed carrier generation would give results indistinguishable from those of pure injection for both gain and excess noise. By contrast a reduction in gain and an increase in excess noise with distributed carrier generation is observed in the RCE-APD.

To interpret the mixed injection results a model is used which has previously been shown to predict accurately the avalanche multiplication and noise characteristics of GaAs $p^+ - i - n^+$ and $n^+ - i - p^+$ diodes. This model has been described in detail in [6] for the case of pure electron (hole) injection and is developed here to predict the noise produced from mixed carrier injection. An ideal $p^+ - i - n^+$ structure is assumed, with a uniform high field region in $0 < x < w$ and no depletion into the p^+ and n^+ cladding regions. Newly generated electrons (holes), produced either by injection into the high field region or as by products of impact ionization, travel in the electric field, ε , a distance d_e (d_h), equal to their dead space, before they are able to ionize. The dead space values are taken as:

$$d_e = E_e / e\varepsilon \quad (1a)$$

$$d_h = E_h / e\varepsilon \quad (1b)$$

where $E_e = 2.3 \text{ eV}$ ($E_h = 2.1 \text{ eV}$) is the ionization threshold energy for electrons (holes) and e is the unit of electronic charge. Following the dead space, the carrier ionization behavior is described by an exponentially decaying spatial probability distribution function (PDF) for ionization path length, x , corresponding to the ionization coefficients α^* and β^* as in [6]. The PDF is thus given by

$$h_e(x) = \begin{cases} 0, & x < d_e \\ \alpha^* \exp(-\alpha^*(x - d_e)), & x \geq d_e \end{cases} \quad (2)$$

for electrons. An expression for the hole PDF for ionization path length, $h_h(x)$, is obtained by replacing d_e and α^* with d_h and β^* .

The values of α^* and β^* are found from the relationships [10]

$$\alpha^{-1} = d_e + \alpha^{*-1} \quad (3a)$$

$$\beta^{-1} = d_h + \beta^{*-1} \quad (3b)$$

and the experimental ionization coefficients, α and β . These are taken from the work of Bulman *et al.* [11] for $\varepsilon > 600 \text{ kV/cm}$, and from the work of Millidge *et al.* [12] for $\varepsilon > 600 \text{ kV/cm}$ with β set equal to α . α and β are interpolated around $\varepsilon = 600 \text{ kV/cm}$ to produce a smooth transition from the data of Bulman to Millidge. The coupled integral (10) and (11) from [6] are then used to calculate the mean gain, and (18) and (19), also from [6], are used to calculate the excess noise. These coupled equations are discretized on a suitable mesh and the resulting linear simultaneous equations are solved to deduce the mean multiplication, $m(x)$, and the excess noise factor, $F(x)$, for a primary electron-hole pair created at position x in the high field.

In the RCE-APD structure photons are absorbed throughout the high field region at a rate given by the function $G(x)$. Using the solutions for $m(x)$ and $F(x)$, the total multiplication, M_T , and total excess noise, F_T , for any spatially distributed generation rate of carrier pairs can be derived.

For a nonavalanching photodiode, the noise spectral density from primary carriers generated in an element dx , due only to shot noise, is given by

$$dN_s(x) = 2e[G(x)e dx] \quad (4)$$

where $e =$ the unit of electron charge.

In the case of an avalanching photodiode, where the primary current is generated throughout the avalanche region before being collected at the device terminals, the spectral noise current density is multiplied by $m^2(x)$ and given by

$$dN_{ms}(x) = 2e[G(x)e]m^2(x) dx. \quad (5)$$

However, the above equation treats $m(x)$ purely as a gain term and does not allow for the fact that $m(x)$ is stochastic in nature. To do so, the excess noise factor for an electron hole pair generated at position x is introduced, which gives

$$dN_T(x) = 2e[G(x)e]m^2(x)F(x) dx. \quad (6)$$

To find the total noise due to the distributed generation of primary carriers we integrate over the avalanche region giving

$$N_T = 2e^2 \int_0^w [G(x)m^2(x)F(x)] dx. \quad (7)$$

The multiplication is defined by the total multiplied output current divided by the total unmultiplied input current and given by

$$M_T = \frac{\int_0^w G(x)m(x) dx}{\int_0^w G(x) dx}. \quad (8)$$

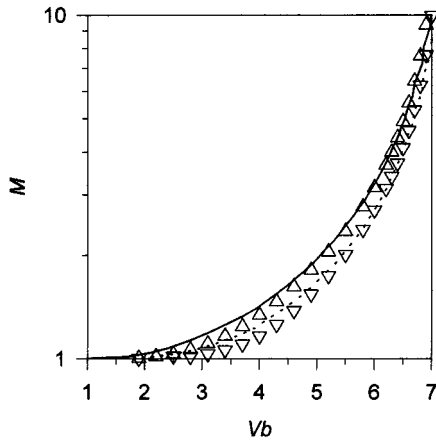


Fig. 4. Multiplication versus reverse bias for the RCE-APD at incident light wavelengths of 442 nm (—, Δ) and 633 nm (---, ∇). Lines represents calculations and symbols the experimental results.

An ideal APD would therefore produce a noise power spectral density, due only to multiplied shot noise, of

$$N_{\text{ideal}} = 2e i_{\text{pr}} M_T^2 = 2e^2 M_T^2 \int_0^w G(x) dx. \quad (9)$$

Hence, the excess noise factor for a distributed generation of carriers is

$$F_T = \frac{N_T}{N_{\text{ideal}}} = \frac{\int_0^w G(x) m^2(x) F(x) dx}{M_T^2 \int_0^w G(x) dx}. \quad (10)$$

The modeled and experimental multiplication and noise characteristics of the RCE-APD are plotted in Figs. 4 and 5 for the cases of pure electron initiated multiplication (442 nm) and for a distributed generation rate of carriers in the high field region (633 nm). The generation rate for mixed injection is taken as $G(x) \propto \exp(-\phi x)$, where $\phi = 4.28 \times 10^4 \text{ cm}^{-1}$ is the absorption coefficient of GaAs at 633 nm [7].

It can be seen in Figs. 4 and 5 that the modeled multiplication and noise characteristics (solid symbols) match closely the measured results (open symbols). The modeled results are slightly higher, possibly because of the simplified choice of PDF in (2). To explain the reason for the higher noise characteristic in the case of mixed injection, plotted in Fig. 6(a) is the multiplication, $m(x)$, and excess noise, $F(x)$, for an electron hole pair injected at a position x at an electric field of 750 kV/cm at which α and β are equal.

Fig. 6(a) includes the special cases of pure electron initiated multiplication, $M_e = m(0)$ and $F_e = F(0)$, and of pure hole initiated multiplication, $M_h = m(w)$ and $F_h = F(w)$. As the position, x , at which an electron-hole pair is created is moved into the high field region the multiplication initially decreases, falling to a minimum value at $x = 28 \text{ nm}$. Thereafter, it rises to a peak close to the middle of the avalanche region, at $x \sim 50 \text{ nm}$ and then falls again, reaching a second minimum at $x = 70 \text{ nm}$. Finally, the multiplication rises to the value of M_h at $x = w = 100 \text{ nm}$. This result contrasts with the local model [13] in which $m(x)$ is independent of position when $\alpha = \beta$. The two minima, one at 28 nm and the other at 70 nm, correspond to the hole and electron dead space distances from the edges of

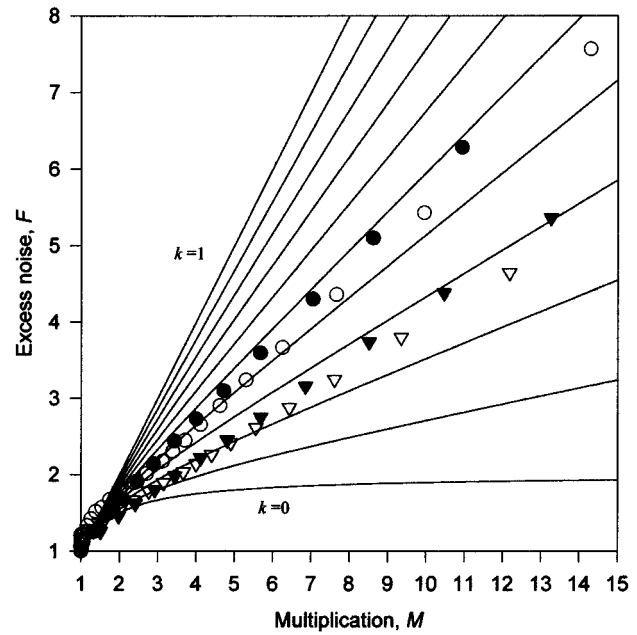


Fig. 5. Excess noise factor versus multiplication for the RCE-APD at incident light wavelengths of 442 nm (∇ , \blacktriangledown) and 633 nm (\circ , \bullet). Open symbols are the measurements and solid symbols the modeled results. Solid lines are as in Fig. 3.

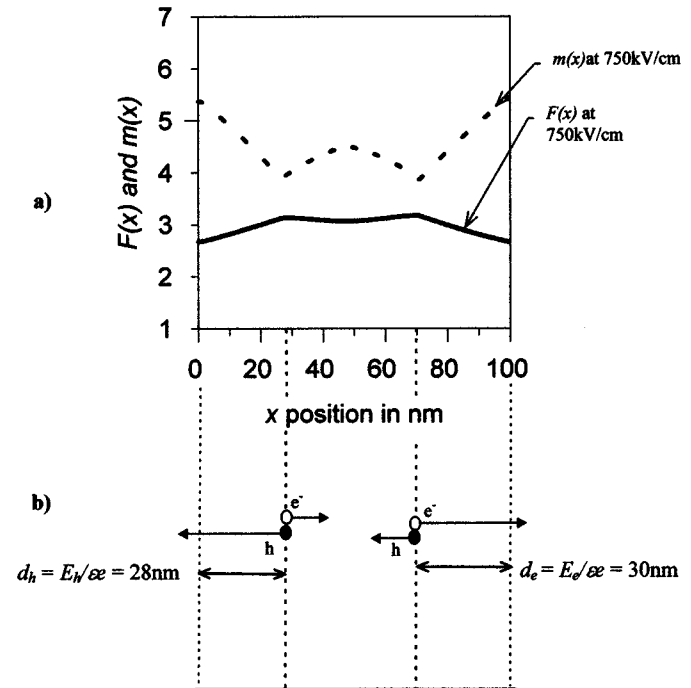


Fig. 6. (a) Multiplication $m(x)$ and excess noise, $F(x)$ for an electron hole pair generated at a position x in the high field region ($0 < x < w$) at an electric field of 750 kV/cm. (b) Schematic of an electron hole pair generated at $x = 28 \text{ nm}$ and $x = 70 \text{ nm}$.

the high field region. As depicted in Fig. 6(b), if an electron-hole pair is created at $x \leq 28 \text{ nm}$ only the electron contributes to multiplication since the hole will leave without ionizing, similarly if an electron-hole pair is generated at $x \geq 70 \text{ nm}$, only the hole contributes to multiplication while the electron leaves without ionizing. Hence, at these minima multiplication is reduced because only one carrier type can go on to ionize and contribute

to multiplication. Consequently, a distributed generation of primary carriers in the high field produces a lower multiplication for the same electric field than pure electron or hole injection.

The excess noise, $F(x)$, is shown in Fig. 6(a) and also depends on the primary carrier injection position x . At $\varepsilon = 750$ kV/cm it is lowest when $x = 0$, $x = w$ and $x = 50$ nm and higher at $x = 28$ nm and $x = 70$ nm, the electron and hole dead space separation, respectively, from the edge of the high field region. This contrasts with the predictions of McIntyre's local noise model [8] in which $F(x)$ is independent of position when $\alpha = \beta$. A distributed generation of carriers in the high field region will therefore produce a worse noise characteristic than either pure electron or pure hole injection.

V. CONCLUSION

In thin GaAs avalanche regions ($\sim 0.1 \mu\text{m}$) a distributed generation of primary carriers in the high field region is found to produce lower gain and higher noise than obtained with pure electron or pure hole initiated multiplication. The implications for device design are that it is still necessary to ensure pure carrier injection for the lowest noise in such structures. However, even in the case of mixed injection, the noise in thin structures still compares favorably with that achievable in thick ($\sim 1 \mu\text{m}$) GaAs avalanche regions. Reducing the absorption-multiplication width further in the RCE-CAM-APD should further decrease the excess noise but an increase in dark current due to tunneling will prove to be a limiting factor.

ACKNOWLEDGMENT

The authors would like to thank G. Diestel for assistance with the characterization and P. N. Robson for many useful discussions.

REFERENCES

- [1] C. Hu, K. A. Anselm, B. G. Streetman, and J. C. Campbell, "Noise characteristics of thin multiplication region GaAs avalanche photodiodes," *Appl. Phys. Lett.*, vol. 69, pp. 1387–1392, 1993.
- [2] K. F. Li *et al.*, "Avalanche multiplication noise characteristics of thin GaAs p-i-n diodes," *IEEE Trans. Electron Devices*, vol. 45, pp. 2102–2107, Oct. 1998.
- [3] D. S. Ong *et al.*, "A Monte Carlo investigation of multiplication noise in thin p⁺-i-n⁺ GaAs avalanche photodiodes," *IEEE Trans. Electron Devices*, vol. 45, pp. 1804–1810, Aug. 1998.
- [4] H. Nie *et al.*, "High speed resonant cavity separate absorption and multiplication avalanche photodiodes with 130 GHz gain bandwidth product," *Appl. Phys. Lett.*, vol. 70, pp. 161–168, 1997.
- [5] H. Nie *et al.*, "Resonant-cavity separate absorption, charge and multiplication avalanche photodiodes with high speed and high gain-bandwidth product," *IEEE Photon. Technol. Lett.*, vol. 10, pp. 409–411, 1998.
- [6] M. M. Hayat, B. E. A. Saleh, and M. C. Teich, "Effect of dead space on gain and noise of double carrier multiplication avalanche photodiodes," *IEEE Trans. Electron Devices*, vol. 39, pp. 546–552, Mar. 1992.
- [7] D. E. Aspnes and A. A. Studna, "Dielectric functions and optical parameters of Si, Ge, GaP, GaAs, GaSb, InP, InAs, and InSb from 1.5 to 6 eV," *Phys. Rev. B.*, vol. 27, pp. 1985–1009, 1983.
- [8] R. J. McIntyre, "Multiplication noise in uniform avalanche diodes," *IEEE Trans. Electron Devices*, vol. ED-13, pp. 164–168, Jan. 1966.
- [9] S. A. Plimmer *et al.*, "Investigation of impact ionization in thin GaAs diodes," *IEEE Trans. Electron Devices*, vol. 43, pp. 1066–1072, July 1996.
- [10] A. Spinelli, A. Pacelli, and A. L. Lacaita, "Dead space approximation for impact ionization in silicon," *Appl. Phys. Lett.*, vol. 69, pp. 3707–3709, 1996.

- [11] G. E. Bulman, V. M. Robbins, and G. E. Stillman, "The determination of impact ionization coefficients in (100) Gallium Arsenide using avalanche noise measurements and photocurrent multiplication measurements," *IEEE Trans. Electron Devices*, vol. ED-32, pp. 2454–2466, Nov. 1985.
- [12] S. Millidge, D. C. Herbert, M. Kane, and D. R. Wight, "Non-local aspects of breakdown in pin diodes," *Semicond. Sci. Technol.*, vol. 10, pp. 344–347, 1995.
- [13] G. E. Stillman and C. M. Wolfe, "Avalanche photodiodes," in *Semiconductor and Semimetals*, R. K. Willardson and A. C. Beer, Eds. New York: Academic, 1977, vol. 12, pp. 291–393.

Kim F. Li (M'99) was born in London, U.K. He received the B.Eng. (Hons.) degree in electronics from the Department of Electronic and Electrical Engineering, University of Sheffield, Sheffield, U.K., in 1995. In 1999 he received the Ph.D. degree in electronic engineering working on avalanche photodiode noise at the same university.

Currently, he is pursuing a career in mixed signal VLSI chip design at Silicon Systems Limited (SSL), Dublin, Ireland.

Duu S. Ong received the B.Sc. (Hons.) degree from the Department of Physics and the M.Phil. degree from Institute of Advanced Studies, University of Malaya, Malaysia, in 1992 and 1995, respectively. In 1998 he received the Ph.D. degree in the Department of Electronic and Electrical Engineering, University of Sheffield, U.K., working on a theoretical study of avalanche multiplication and noise in avalanche photodiodes.

He is currently a Senior Lecturer in the Faculty of Engineering, Telekom University, Malaysia.

John P. R. David (SM'96) received the B.Eng. and Ph.D. degrees from the Department of Electronic and Electrical Engineering, University of Sheffield, Sheffield, U.K., in 1979 and 1983, respectively.

In 1983, he joined the Department of Electronic and Electrical Engineering, University of Sheffield, where he worked as a Research Assistant investigating impact ionization. In 1985, he became responsible for characterization within the SERC (now EPSRC) Central Facility for III–V Semiconductors at the same university. His current research interests are piezoelectric III–V semiconductors and impact ionization in bulk and multi-layer structures.

Richard C. Tozer (SM'98) received the B.Eng., M.Eng., and Ph.D. degrees from the University of Sheffield, Sheffield, U.K., in 1970, 1972, and 1975, respectively.

Following a period of postdoctoral research at the University of Sheffield in the area of CCD device applications, he became a Lecturer at the University of Essex, U.K., where he researched active sound cancellation. In 1980, he returned as a lecturer to Sheffield where he teaches analogue circuit design. His research interests involve the application of analogue circuits to a wide range of experimental and instrumentation problems.

Graham J. Rees received degrees in physics and theoretical physics from Oxford University, Oxford, U.K., and Bristol University, Bristol, U.K.

He has since been with Rome Università della Scienze, Imperial College London, Plessey (now GEC) Caswell, Lund University, Sweden, and Oxford University. He is currently a Professor at the University of Sheffield, Sheffield, U.K. His interests are in the physics of semiconductors and devices.

Stephen A. Plimmer was born in Stoke-on-Trent, U.K., in 1972. He received the B.Sc. (Hons.) degree in physics and the Ph.D. degree in electronic engineering from the University of Sheffield, U.K., in 1993 and 1997, respectively. His doctoral work focused on experimental and theoretical study of impact ionization in $\text{Al}_x\text{Ga}_{1-x}\text{As}$ ($x = 0 - 0.9$).

He now works as a Research Associate at the University of Sheffield, where his main topic is single photon avalanche detectors (SPAD's).

Keng Y. Chang, photograph and biography not available at the time of publication.

John S. Roberts, photograph and biography not available at the time of publication.